090703

26. Space-Weather Effects on Transionospheric Radio Wave Propagation

A. Bhattacharyya[1] *and S. Basu*[2]

[1]Indian Institute of Geomagnetism
Colaba, Mumbai 400005, India
Tel: +91-22-215 1607; Fax: +91-22-218 9568; E-mail: archana@iig.iigm.res.in

[2]Air Force Research Laboratory, Space Vehicles Directorate
Hanscom AFB, MA 01731-3010, USA
Tel: +1 (781) 377-3078; Fax: +1 (781) 377-3550; E-mail: Santimay.Basu@hanscom.af.mil

1. ABSTRACT

Space weather affects the distribution of plasma in the ionosphere and plasmasphere through which radio waves used for communication and navigation propagate. On some occasions, only large-scale (> 10 km) structures in the propagation medium are encountered by the radio waves, while at other times, small-scale variations in ionospheric electron density give rise to scintillations on transionospheric radio waves. Recent studies of both of these situations at equatorial, mid- and high latitudes are reviewed.

2. INTRODUCTION

The concept of "space weather" is now widely used in quantitative descriptions of the physical changes in the near-Earth space environment in response to variations in solar radiation, solar plasma ejection, and the electromagnetic status of the interplanetary medium. Even as answers are being sought to questions related to the parameters required for an adequate description of space weather, it is recognized that one of the most important effects of space weather, which has a bearing on operational systems, is that on transionospheric radio wave propagation. Basically, radio wave pulses are modified as a result of dispersion and scattering in the medium of propagation [*Yeh and Liu, 1979*]. Space-weather-related changes in the electron-density distribution in the path of a signal due to production or loss processes, electrodynamics of the intervening plasma, and changes in the neutral component that affect the plasma, alter the propagation medium and, hence, its effect on a radio wave signal. In the last decade, the utility of radio wave transmissions from the Global Positioning System (GPS) satellites in obtaining information about the Earth's ionosphere simultaneously from a global network of stations has been demonstrated. To lowest order, changes in the total electron content (TEC) along the signal path – on transverse spatial scales far in excess of the Fresnel scale, which is determined by the signal frequency – contribute to only an excess time delay. For an undisturbed ionosphere, where the electron density does not vary significantly over short (< 500 m) scale lengths, this is the only effect that the ionosphere has on GPS signals.

The scattering of radio waves enters the picture when spatial scales of electron-density variations, in a direction transverse to the signal path, are of the order of or smaller than the Fresnel scale. As a result of scattering, a diffraction pattern is formed in the plane of the receiver. Movement of the irregularities across the signal path results in temporal fluctuations or scintillations in the amplitude and phase of the signal recorded by a receiver. The severity of scintillation effects is determined by the power spectrum of electron-density variations in the propagation medium and the orientation of the signal path. Space weather influences the development of small-scale irregularities in the ionospheric plasma, which may give rise to scintillations on transionospheric VHF, UHF, and even-higher-frequency radio waves. The ionosphere in the equatorial and polar-cap/auroral regions, in particular, often exhibit such departures from an undisturbed, smooth state. Dual-frequency GPS observations have provided a unique opportunity to simultaneously study the scintillations caused by ionospheric refractive-index variations and the fluctuations in the TEC along the signal path, which directly represent electron-density variations associated with the scintillation-producing irregularities. Radio wave signals, transmitted from geostationary satellites and recorded by spaced receivers, yield information about the dynamics of ionospheric irregularities, which are affected by space weather. Recent studies of seasonal, solar-cycle, and magnetic-activity-linked variations in TEC and ionospheric scintillations are reviewed here.

As far as forecasting the impact of space weather on transionospheric radio wave propagation is concerned, monitoring of large-scale plasma-density structures in the ionosphere is of major importance. The technique of computerized ionospheric tomography (CIT) is now well developed for studying such ionospheric structures [*Leitinger, 1999*; *Andreeva et al., 2001*]. Some results obtained with this technique, which have been reported during the years 1999-2001, are briefly outlined in the present review.

3. GPS-BASED OBSERVATIONS OF TEC

Data from the International GPS Service for geodynamics (IGS) network of over 200 GPS signal-receiving ground-based stations have been a boon for scientists studying space-weather effects on transionospheric radio propagation. The GPS observables are the ranges deduced from measured time or phase differences, obtained by comparison between received and receiver-generated signals. Hence, the ranges are biased by satellite and receiver clock errors. Also, the total electron content along the slant path of a signal introduces an excess time delay for the signal reaching the ground receiver. Hence, the term "pseudo-range" is used for the range derived from GPS measurements. The intervening plasma being a dispersive medium, the dual-frequency transmissions on L1 (1.57 GHz) and L2 (1.23 GHz) are affected to different extents. This allows determination of an "ionospheric correction" when a dual-frequency receiver is used to record the GPS signals. The carrier-phase measurements have an accuracy of 0.01 cycles or better [*Hofman-Wellenhof et al., 1994*]. However, the differential carrier-phase measurements, using dual-frequency observations, yield only the relative slant TEC (STEC) along the signal path, uncertain to an additive constant. The pseudo-range or group-delay measurements, although more noisy, provide an absolute measure of the STEC in terms of the range error in meters. In order to derive a more accurate estimate of the absolute value of STEC, the differential carrier-phase measurements are fitted to the pseudo-range estimates, using data from the middle of the satellite pass to avoid multipath effects, which are present at low elevation angles. In most studies, the TEC derived from dual-frequency GPS signals have been identified with the ionospheric electron content (IEC). In recent years, a great deal of effort has gone into developing new methods to derive ionospheric parameters from GPS data [*Mannucci et al., 1998*]. A commonly used approximation to estimate the vertical TEC from $\bar{S}$TEC is the "Shell model," in which it is assumed that the plasma distribution in the intervening medium depends on altitude alone [*Mannucci et al., 1999*]. This approximation fails in the presence of significant horizontal gradients in electron density. Nevertheless, such approximations continue to be used in studying the effects of geomagnetic storms and substorms on the TEC, and, hence, on GPS measurements.

3.1 Ionospheric Delay Models

For the more commonly used single-frequency receiver of GPS signals, "ionospheric corrections" are estimated on the basis of a model of ionospheric electron content – like that of *Klobuchar* [*1987*] – broadcast by the GPS satellites. This model provides almost a 50% reduction in ionospheric error in positioning, under quiet geomagnetic conditions at mid-latitudes, in the absence of significant ionospheric irregularities. The accuracy of this model is lower under disturbed geomagnetic conditions in high-latitude and equatorial regions. There are also purely GPS-data-based methods for modeling the ionospheric delay (ID) under different space-weather conditions. These may rely on a dense network of single-frequency GPS receivers [*Rocken et al., 2000*], or on updating the global ionospheric delay model by fitting the parameters of Klobuchar's model with the use of measured values obtained from a dual-frequency receiver at a reference station [*Afraimovich et al., 2000*]. While the former technique claims to provide better GPS surveying results than dual-frequency networks, even during solar-maximum conditions, the latter method reduces the ionospheric rms error in determining positions for a local differential-systems user by a factor of about two for magnetic-storm conditions and solar-eclipse conditions. A method has been developed for extrapolating electron-density measurements from incoherent-scatter radar to GPS altitudes, with temperature inputs from the Sheffield University plasmasphere-ionosphere model, SUPIM [*MacPherson et al., 2000*]. The TEC estimated in this manner has been compared with the TEC derived from GPS observations during both quiet and magnetically disturbed periods, and this has paved the way for use of the extrapolation technique in quick and accurate calibration of nearby GPS receivers [*Makela et al., 2000*].

There are several self-consistent, physical models of the ionosphere-thermosphere system, and other ionospheric models in which the thermospheric parameters are provided by empirical inputs, which are applicable to low-, middle-, and high-latitude regions [*Bailey and Balan, 1996*; *Anderson et al., 1998*; *Webb and Essex, 2000*]. Since these models are useful for estimating excess time-delay corrections to GPS measurements, it is important to determine their reliability under different space-weather conditions. *Anderson et al.* [*1998*] have compared five such models with data obtained in mid-latitude regions from incoherent-scatter radar and digisonde observations under geomagnetically quiet conditions, during both summer and winter solstices at solar maximum and minimum. They conclude that for reliable quantitative predictions, data-assimilation techniques need to be introduced in the development of global ionospheric models.

3.2 Protonospheric Contribution

With a GPS satellite orbiting at an altitude of 20,200 km, the error in pseudo-range, which arises from the STEC, includes contributions from ionospheric electrons as well as plasmaspheric or protonospheric electrons. The largest contribution to STEC comes from the *F* layer of the ionosphere. Hence, most of the modeling efforts have been concerned with this region. Nevertheless, in order to study the effect of space weather on GPS signals, it is important to model the contribution of the hydrogen-dominated plasma of the high plasmasphere or protonosphere to the STEC under different space-weather conditions. *Lunt et al.* [*1999a*; *1999b*] have addressed this problem by using SUPIM [*Bailey and Balan*, *1996*] to compute the diurnal variation of equivalent vertical electron content, integrated to an altitude of 1100 km and to the GPS satellite altitude, at the extremes of the solar cycle. The difference between the two represents the protonospheric electron content (PEC). The altitude of the Navy Ionospheric Monitoring Satellites (NIMS), which provided estimates of the ionospheric electron content, dictated their choice of an altitude of 1100 km for the ionosphere. This was used to determine the PEC experimentally [*Lunt et al.*, *1999c*]. Such calculations for receiving stations at mid-latitudes in the European and American sectors showed that during solar minimum, the PEC may be 50% of the total at night at 0° longitude, while at 90° W longitude, this part is around 23%. The geometries of the ray path and plasmaspheric flux tubes are important factors in determining the contribution of PEC to GPS measurements. Model calculations for these sectors [*Lunt et al.*, *1999a*] show that in going from solar minimum to maximum, the protonospheric contents are typically doubled in absolute magnitude. However, the protonospheric contribution as a percentage of the TEC is reduced during solar maximum. As far as positional accuracy obtained from single frequency (L1) GPS receivers is concerned, a change in STEC of 6.15 TECU (1 TECU = 10^{16} m^{-2}) corresponds to an error of 1 m. Hence, in absolute terms, the protonospheric contribution to single-frequency positional error in the European sector may not be much greater than a meter throughout the solar cycle, provided elevation angles due south of the station are greater than 50°.

The TOPEX/POSEIDEN data, which provides ionospheric electron content estimates over the oceans, has been used to confirm the mid-latitude nighttime TEC increase that was found from GPS observations [*Horvath and Essex*, *2000*]. Their results indicate that the development of the mid-latitude nighttime peak coincided with the breakdown of the equatorial anomaly due to reversal of the vertical $\mathbf{E} \times \mathbf{B}$ drift. Thus, a westward electric field is believed to be the main driving mechanism for plasma flow from the plasmasphere to the ionosphere.

3.3 Geomagnetic Storm Effects

Depletion of the plasmaspheric flux tubes during geomagnetic storms and their subsequent recoveries have also been shown in the investigations of *Lunt et al.* [*1999d*]. Ground magnetometer observations have suggested that convection caused by the strong electric field associated with a magnetic storm could erode the plasmasphere as low as $L = 2$ [*Chi et al.*, *2000*]. The TEC inferred by GPS signals recorded at Boulder, Colorado, also showed a sizable decrease during this storm, which is attributed to a decrease in the ionospheric electron content (IEC) due to lower efficiency of ionization by solar EUV radiation [*Fuller-Rowell et al.*, *1997*]. The effect of a lower IEC on the depletion and refilling of the plasmasphere is not yet known.

Several case studies of the observed effects of geomagnetic storms [*Aarons and Lin*, *1999; Aponte et al.*, *2000*; *Chi et al.*, *2000*; *Kelley et al.*, *2000*; *MacPherson*, *2000*; *Mendillo et al.*, *2000*; *Basu et al.*, *2001a*; *2001b*] and solar flares [*Afraimovich*, *2000*] on the STEC along the satellite-to-receiver path give an idea of the various possibilities that exist. *Mendillo et al.* [*2000*] – in the first study of magnetic storm effects on TEC at equatorial latitudes, using GPS data – compared the average daily variation of vertical TEC at six stations for three magnetically quiet days (average Ap = 3) in October, 1996, with those for three magnetically disturbed days (Average Ap = 34) in the same month. These six stations span the equatorial region, extending up to the Appleton anomaly. The data here were limited to just three magnetically active days and, therefore, the results may not be representative of general storm-time morphologies at equatorial latitudes. However, they indicate that at low latitudes, it is difficult to distinguish magnetic-storm effects

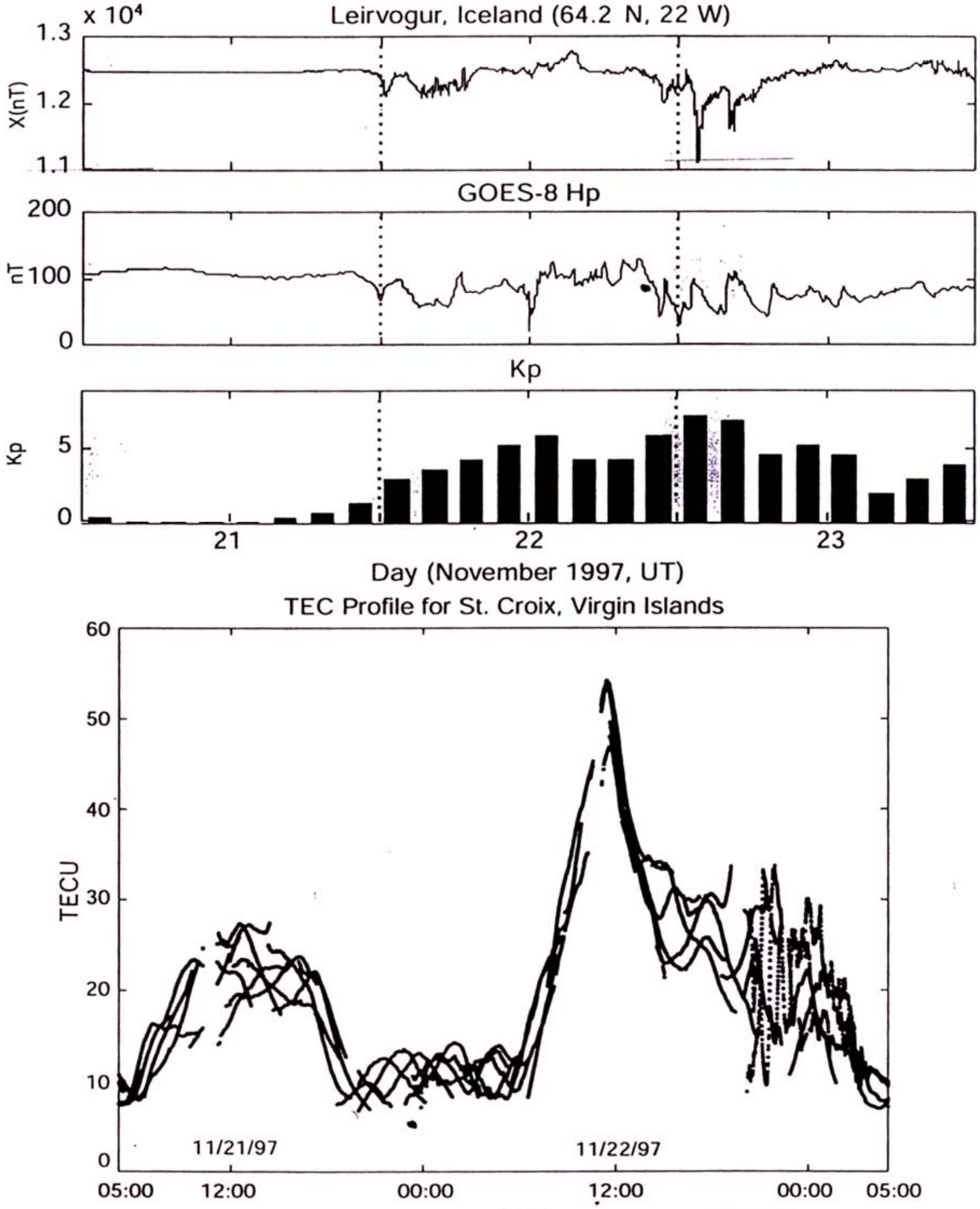

Figure 1. The top three panels show, respectively, the pole-ward component of the magnetic field, measured at Leirvogur, Iceland (top); data from the fluxgate magnetometer on the geostationary satellite GOES-8, which is located at 75° W longitude (middle); Kp indices for the same period. The bottom panel shows the total equivalent vertical electron content (1 TECU = 10^{16} m^{-2}) for all GPS satellites in view from St. Croix near Puerto Rico on November 21-22, 1997; LT = UT – 4 hours [after *Kelley et al., 2000*].

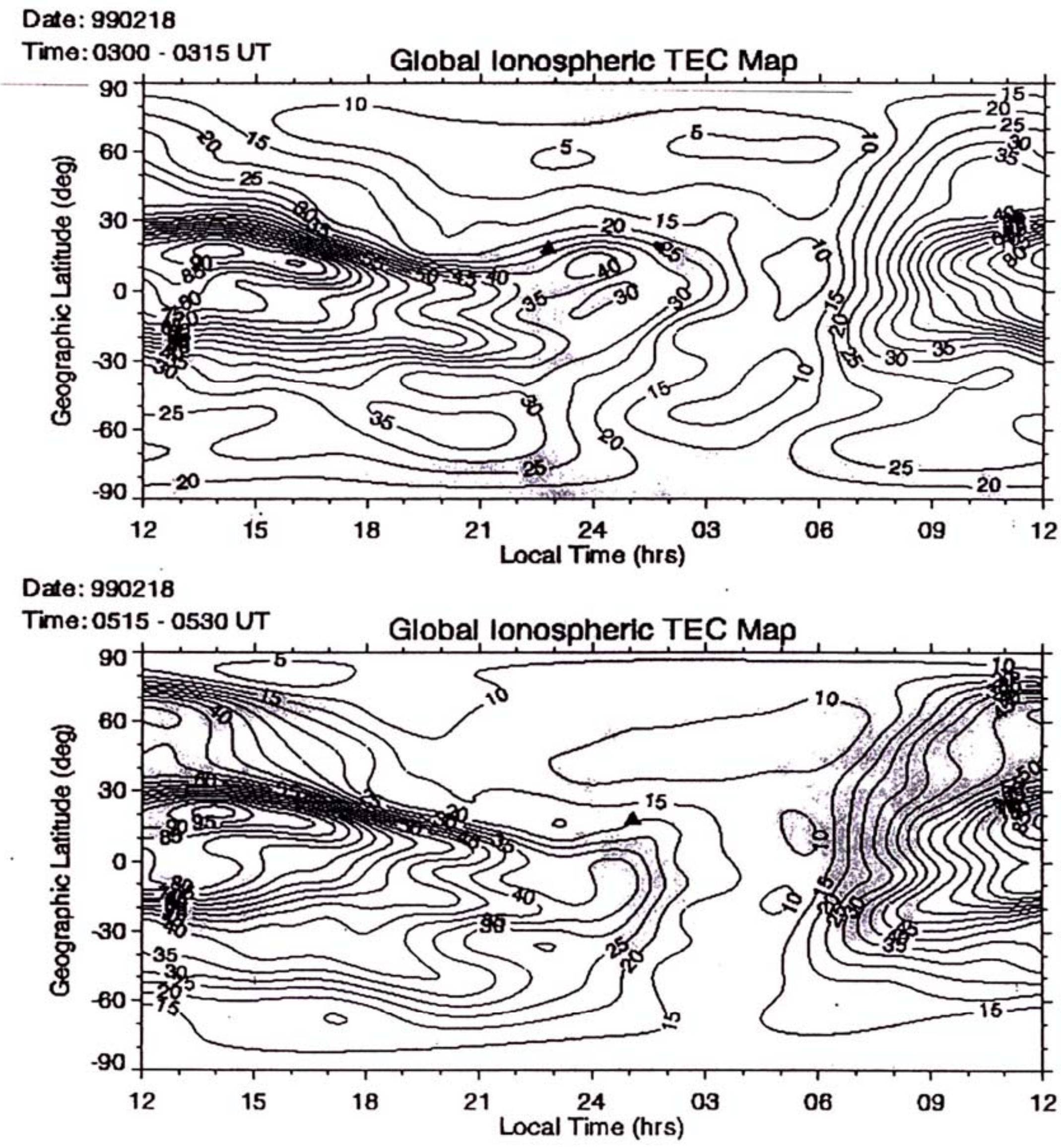

Figure 2. Global TEC maps at 0300 and 0515 UT on February 18, 1999, derived from GPS data. The top panel shows the increase in TEC in the Caribbean sector to 30-35 units southeast of Arecibo, due to a poleward expansion of the equatorial anomaly during a large geomagnetic storm (Kp ≥ 5). The bottom panel shows lower TEC after the anomaly receded [after *Aponte et al., 2000*].

because of the large variability found during quiet times. In their study of the response of the equatorial ionosphere in the South Atlantic region to the great magnetic storm of July 15, 2000, *Basu et al.* [*2001a*] reported that GPS measurements at Fortaleza (dip latitude = 4.5°) showed a precipitous fall in TEC. Combined DMSP satellite and ground GPS observations indicated that the ionospheric plasma was not only lifted above 840 km, which is the altitude of the DMSP satellite, but was also transported away from this region. Such deep and latitudinally extended depletions are believed to be features of the Brazilian sector, alone [*Basu et al., 2001a*].

The storm-time effect on the equivalent vertical TEC derived from GPS observations at a mid-latitude station near Puerto Rico has been found to be much more dramatic [*Kelly et al., 2000*; *Makela et al., 2001*]. The Kp indices for a period covering the beginning and progression of a magnetic storm in November, 1997, are shown in Figure 1, which also shows the behavior of the equivalent vertical TEC derived for all GPS satellites in view from Isabela on November 22, 1997. This day, with strong geomagnetic activity, may be compared with the previous day, which was magnetically quiet. It is seen that as the storm developed, the equivalent vertical TEC became almost twice as large on the dayside as during a quiet period, and continued to remain elevated in the post-sunset period. During periods of large geomagnetic disturbances, both the Arecibo incoherent-scatter radar (ISR) and ionosonde have recorded large enhancements in peak electron density and *F2* peak height in the nighttime ionosphere, with electron density near midnight rising to daytime values during one event. TEC maps from GPS for this night, shown in Figure 2, confirmed that a pole-ward expansion of the equatorial anomaly resulted in the observed density enhancements [*Aponte et al., 2000*]. The TEC derived using GPS data from the IGS network in Europe and three North American stations, during the January 6-11, 1997, storm, indicated large deviations from the average behavior, particularly at high latitudes in the night-side/early-morning sector [*Jakowski et al., 1999*]. The observations supported the assumption that an equator-ward propagation of the high-latitude perturbation, guided by thermospheric winds, causes an effective uplifting of plasma on the dayside (positive phase), and a subsequent enhanced plasma loss due to the equator-ward transport of storm-induced composition changes.

4. IONOSPHERIC SCINTILLATIONS

4.1 IRREGULARITIES AND SCINTILLATIONS

Plasma instabilities are the main source for the creation of structures in the equatorial ionospheric plasma, whereas several other processes besides plasma instabilities play a role in the generation of horizontal structures in the plasma density of the high-latitude ionosphere. These two regions are particularly susceptible to the development of irregularities with scale sizes that can give rise to scintillations on GPS signals, which can be severe enough to lead to a loss of receiver lock. Scintillation, which is basically an integrated phenomenon, has a maximum contribution from the region of highest plasma density in the vicinity of the ionospheric *F*-layer peak. As far as scintillation effects on transionospheric radio waves used for communication and navigation are concerned, the intermediate-scale structures, of scale sizes in the range 0.1-10 km, are the most important. For signal frequencies in the VHF or higher range, which are much greater than the plasma frequencies and collision frequencies prevalent in the ionospheric-irregularity region, the variation in ionospheric refractive index is proportional to the variation in electron density.

In a situation where the irregularities are confined to a thin layer, such that the only effect this layer has on radio waves propagating through it is to impose an irregular phase perturbation on it, the layer is treated simply as a phase-changing screen, in the so-called "phase-screen approximation" (PSA) [*Yeh and Liu, 1982*]. As a result of the imposed phase perturbation, variations in amplitude of the radio waves build up as the waves, after emerging from the irregularity layer, propagate in free space to the plane of the receiver. Additional phase fluctuations also appear as the waves propagate in free space. *Bhattacharyya et al.* [*2000*] have used the phase-screen approximation to demonstrate that the phase measured using the GPS receivers is a combination of the original phase perturbation imposed by the irregularities and phase scintillations. They used the example of ionospheric irregularities that are highly elongated along the geomagnetic field lines, as in the case of the irregularities associated with plasma bubbles in the nighttime equatorial ionosphere. These give rise to an initial phase perturbation, $\phi(x)$, which is one-dimensional, depending only on x, the magnetic east-west coordinate:

$$\phi(x) = -\lambda r_e \Delta N_T(x). \tag{1}$$

Here, λ is the signal wavelength, $\Delta N_T(x)$ is the variation in TEC along the signal path, and $r_e \left(= 2.8\times10^{-15}\text{ m}\right)$ is the classical electron radius. For the model irregularity layer used by *Bhattacharyya et al.* [2000], $\Delta N_T(x)$ is shown in Figure 3a. When a plane wave propagates along the z axis, with normal incidence on the phase screen located at $z = 0$, the complex amplitude,

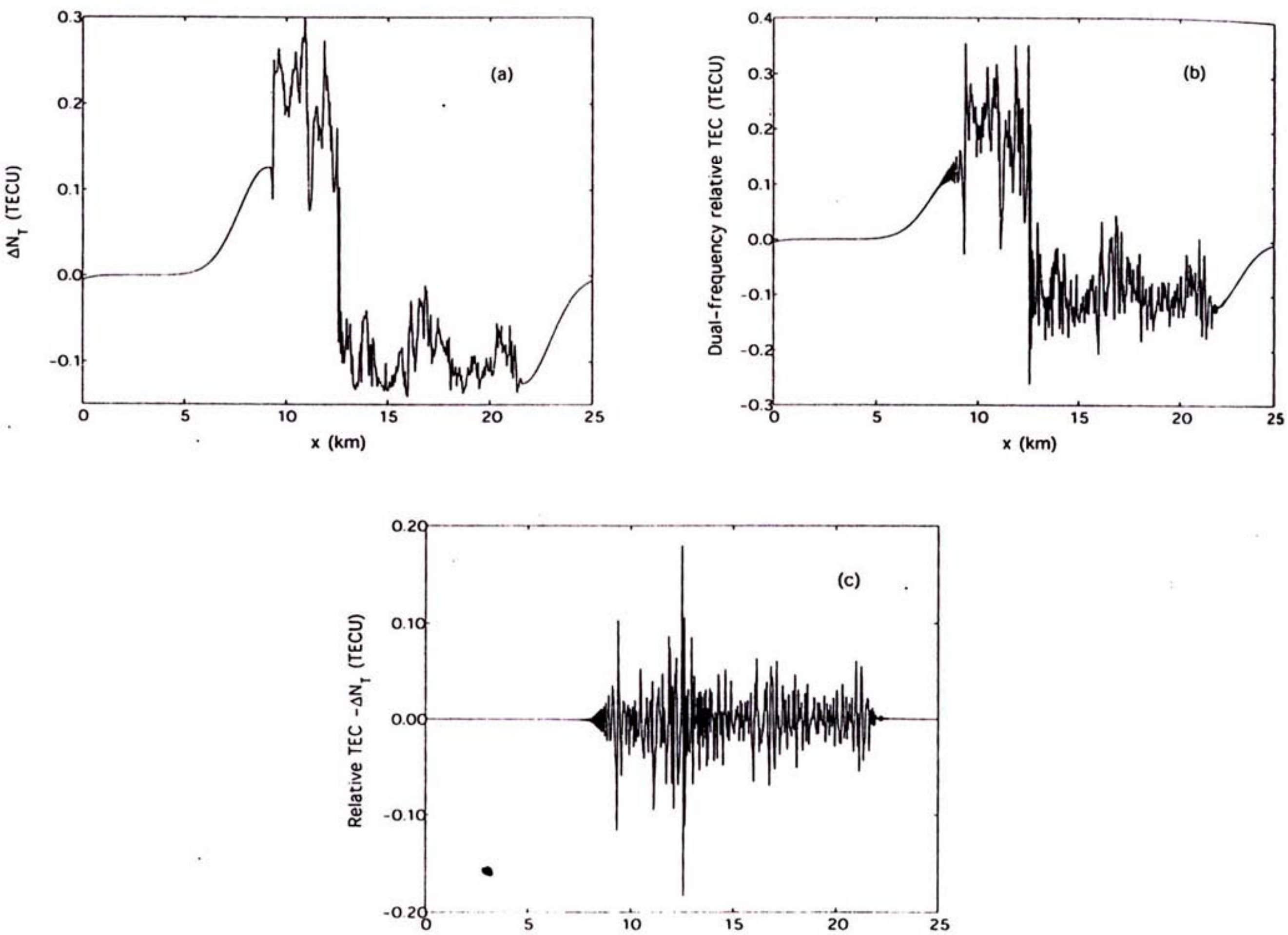

Figure 3. (a) The variation, ΔN_T, along a transverse (x) direction, in TEC along the signal path, for a model irregularity layer of thickness 20 km; (b) The variation in relative TEC that would be obtained from dual-frequency observations of L1 and L2 after the GPS signals propagate through the irregularity layer; (c) The contribution of phase scintillations on L1 and L2 to the relative TEC estimate shown in (b) [after *Bhattacharyya et al.*, 2000].

$u(x, z_R)$, of the wave in the reception plane at a distance z_R from the phase screen, may be obtained from the Fresnel-diffraction result, under the assumption of forward scattering [*Ratcliffe, 1956*]:

$$u(x, z_R) = \sqrt{\frac{i}{\lambda z_R}} \int_{-\infty}^{\infty} u(x', 0) \exp\left[\frac{-i\pi (x - x')^2}{\lambda z_R}\right] dx', \tag{2}$$

where $u(x, 0)$ is the complex amplitude of the radio wave just as it emerges from the phase screen:

$$u(x, 0) = e^{-i\phi(x)}. \tag{3}$$

From Equation (2), it is seen that the phase variation of the radio wave when it reaches the plane of the receiver is different from the initial phase perturbation, $\phi(x)$, and the difference between the two, which may be termed phase scintillations, is not related to ΔN_T in the same manner as $\phi(x)$ is related to ΔN_T. The relative TEC variation that would be obtained from carrier-phase measurements by a dual-frequency receiver of L1 and L2 signals, which propagate through the model layer on their way to the receiver, is determined using Equation (2). This is displayed in Figure 3b. For the receiver, the spatial scales used in these figures are converted to time scales by the drift of the irregularity layer across the signal path. The contribution of phase scintillations on L1 and L2 signals to the measured relative TEC variations is just the difference between the variations in Figure 3a and 3b, which is displayed in Figure 3c. This arises only due to the presence of relatively short-scale-length ($\leq$ the Fresnel scale) irregularities in the layer. This demonstrates the distinction between the effects of large-scale-length variations in TEC on transionospheric radio waves, which were discussed in Section 3, and the effects of short-scale-length variations in TEC, which give rise to scintillations.

4.2 Quantitative Measures of Ionospheric Scintillations

It is imperative to use quantitative measures of scintillation effects in a study of space-weather effects on ionospheric scintillations. The statistical parameter commonly used to quantify the magnitude of scintillation effects is the S_4 index, which is the standard deviation of normalized intensity fluctuations recorded by a receiver over the chosen time interval. The complex structure of ionospheric plasma-density irregularities generally requires that a statistical characterization be used for them, as well. This is done in terms of the space-time correlation function of density fluctuations, or its power spectrum [*Bhattacharyya et al., 1992*]. The temporal structure of scintillations recorded at a single location is determined by the strength of the irregularities, the irregularity power spectrum, and the speed with which irregularities drift across the signal path. The GPS signals have provided a unique opportunity to simultaneously study the short-scale-length variations in STEC along the signal path in the presence of ionospheric irregularities, and the scintillations caused by these irregularities. The widely available GPS data from the IGS network observations consist of 30 s samples. A sampling period of 30 s would generally reveal spatial scales greater than 6 km, when the vector sum of the ionospheric projection of the satellite velocity and irregularity drift transverse to the propagation path has a magnitude of 100 m/s. The Fresnel scale for the GPS L1 signal is about 360 m when the distance between the ionospheric penetration point and ground receiver is 350 km. Since the power spectral density is higher at larger scale lengths, due to a power-law type of irregularity spectrum, for weak to moderate drift of the irregularities across the signal path, the irregularities that are seen in TEC derived from GPS data may imply that irregularities of scale lengths in the neighborhood of the Fresnel scale are also present in the ionosphere, with sufficient strength to cause significant scintillations. At high latitudes, where the ionospheric motion may be as large as 1 km/s, the 30 s sampling interval may correspond to such a large Nyquist scale that a power-law spectrum of density variations could yield too small an irregularity strength at 500 m scale size to cause observable amplitude scintillations on GPS signals. Nevertheless, simultaneous observations of L1 and L2 signals from GPS satellites at intervals of 30 s using dual-frequency receivers have been widely used to study ionospheric irregularities in equatorial as well as high latitudes [*Aarons et al., 1997*; *Pi et al., 1997*; *Basu et al., 1998*; *Aarons et al., 1999a*, *1999b*; *Aarons and Lin, 1999*; *Mendillo et al., 2000*].

A measure of TEC variations derived from the data that may be directly associated with scintillation effects was introduced by *Pi et al.* [*1997*]. This measure is the rate of change of TEC index (ROTI). An example of simultaneous variations in the slant TEC and in intensity scintillations on L1, recorded at Ancon (1.5° dip) at a higher sampling rate of 1 Hz, is shown in Figure 4 [*Beach and Kintner, 1999*]. In order to quantify the relationship between the two variations, *Beach and Kintner* [*1999*] compared the S_4 indices computed from intensity-scintillation data on L1 with the ROTI calculated using simulated IGS data, derived from the relative TEC measurements. Since the 30 s sampling period for the TEC variations represents different spatial scale lengths, depending on the velocity with which the irregularities drift across the signal path, it was pointed out by *Basu et al.* [*1999*] that any quantitative relationship between S_4 and the ROTI must depend on this drift velocity, as well. The nature of a relationship between S_4 and TEC variations was explored by *Bhattacharyya et al.* [*2000*] on the basis of a theoretical relationship between the intensity, I, of the radio wave recorded by a receiver, and the phase variation, $\phi(x)$, imposed on the incident wave by a one-dimensional phase screen [*Bhattacharyya, 1999*]. Equation (1) gives the relationship between $\phi(x)$ and variations $\Delta N_T(x)$ in STEC along the signal path. Using the drift speed, v, of the irregularities relative to the signal path along the x axis, spatial variations along the x direction are converted into temporal variations at the site of the receiver. Any changes in v with time may be ignored over relatively short intervals during the course of a scintillation event. The following equation then describes an approximate relationship between observed variations in TEC and the intensity, $I(t, z_R)$, of the received signal at an instant of time, t :

$$\frac{d^2}{dt^2}\Delta N_T = \frac{-2\pi}{\lambda r_e}\frac{v^2}{\lambda z_R}\left[1-\frac{I(t,z_R)}{I_0}\right]. \tag{4}$$

Here, I_0 is the uniform intensity of the incident wave before it encounters the irregularities. Since the S_4 index is the standard deviation of the normalized intensity, $I(t,z_R)/I_0$, Equation (4) suggests that an index derived from the second derivative, $d^2\Delta N_T/dt^2$, of TEC variations, rather than $d\Delta N_T/dt$, may be a more natural choice as an indicator of scintillation activity. The proportionality factor between this derivative of rate of change of TEC index (DROTI) and the S_4 index depends on both the drift speed, v, of irregularities relative to the signal path, and z_R, the distance of the receiver from the phase screen, in a combination which gives the Fresnel frequency $v_F = v/\sqrt{2\lambda z_R}$, since $\sqrt{2\lambda z_R}$ is the Fresnel scale [*Bhattacharyya et al., 2000*]. Even an approximate quantitative relationship between the S_4 index and TEC variations would be useful in studies of space-weather effects on transionospheric radio signals using the global IGS network.

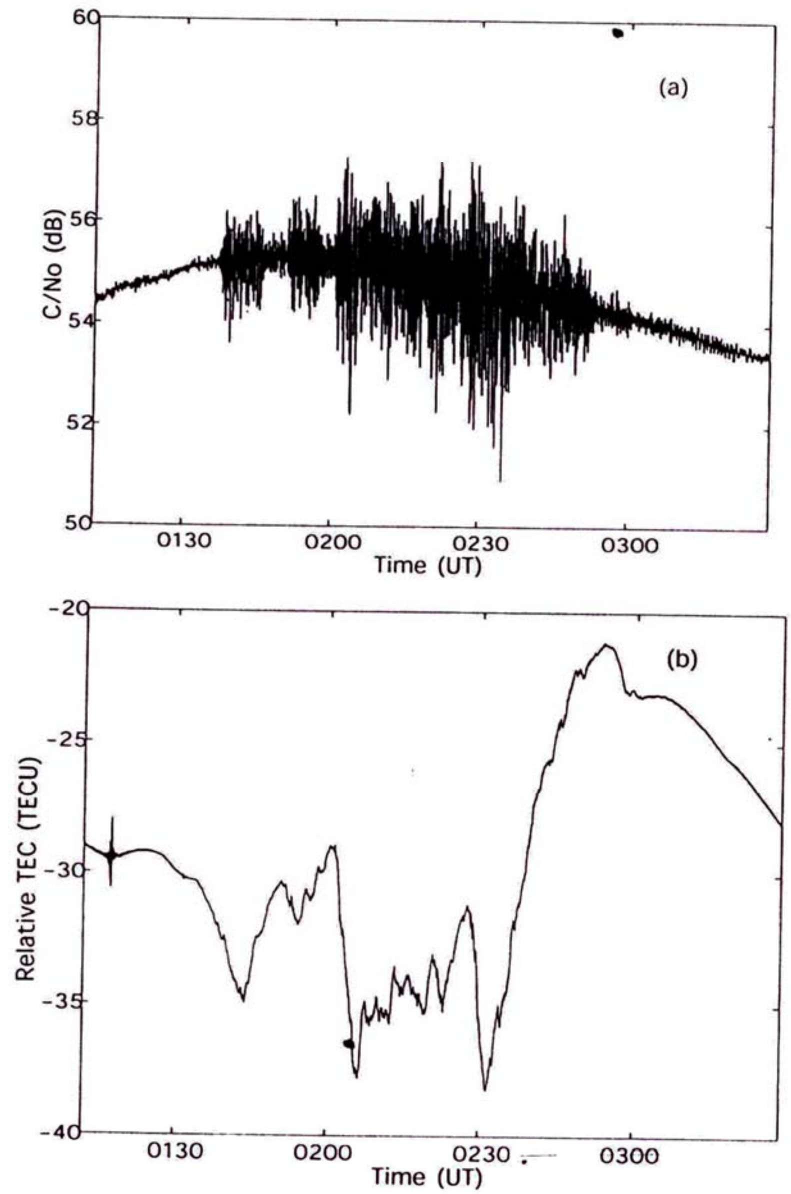

Figure 4. (a) Intensity scintillations on GPS L1, propagating from PRN5 to Ancon; (b) Simultaneous variations in relative TEC along the same signal path, obtained from dual-frequency GPS observations at Ancon on April 9, 1997 [after *Beach and Kintner, 1999*].

4.3 EQUATORIAL SCINTILLATIONS

The post-sunset *F*-region irregularities produce the most severe scintillations in the equatorial region. At the time of sunset, an enhanced eastward electric field generally develops at *F*-region heights [*Fejer et al., 1999*; *Fesen et al., 2000*]. As a result, the ionosphere moves upward, and a steep vertical gradient in plasma density develops on the bottomside of the equatorial *F* region. This configuration is inherently unstable to the Rayleigh-Taylor (R-T) instability [*Kelley, 1989*; *Hysell, 2000*]. After its initiation on the bottomside of the nighttime equatorial *F* region, the instability evolves nonlinearly into large-scale plasma depletions, or bubbles, which may extend to great heights into the topside of the *F* region. The plasma-density variations in the region of the bubbles span a large range of scale sizes, including the intermediate scales ranging from tens of meters to tens of kilometers, which give rise to scintillations on transionospheric radio waves. The day-to-day occurrence pattern of these irregularities is yet to be understood [*Devasia et al., 2002*], but there are studies that have established the seasonal and solar-cycle variations in the occurrence pattern of scintillations due to these irregularities [*Chakraborty et al., 1999*; *Mendillo et al., 2000*]. Also, GPS data has been used to study nighttime equatorial irregularities, which are linked with magnetic activity [*Aarons et al., 1999a*; *1999b*; *Basu et al., 2001b*].

4.3.1 Solar-Cycle Effects

Fejer et al. [*1999*] used long-term radar observations, from 1968 to 1992 at the Jicamarca observatory, located near the dip equator, to study the role played by the equatorial *F*-region vertical plasma drift velocity in the generation and evolution of plasma-density irregularities, which are described by the generic term "Equatorial Spread *F*" (ESF). According to these authors, the presence of necessary conditions for the generation of strong spread *F* during the early night period appears to be linked to the vertical drift velocity being high enough, the threshold value of the drift velocity increasing linearly with solar flux. The influence exerted by the electrodynamic drift of the plasma near the magnetic equator on the distribution of plasma and the evolution of irregularities in the nighttime equatorial ionospheric *F* region has been examined using long-term observations of VHF scintillations at a station near the crest of the equatorial anomaly in the Indian longitude zone. These observations were combined with TEC data obtained at the same station using the Faraday-rotation technique, and with the *F*-layer virtual height variation derived from ionosonde data at an equatorial station in India, for the period 1977-1990 [*Chakraborty et al., 1999*]. On those occasions when the equatorial plasma bubbles rise to an altitude high enough to have the field-aligned irregularities map down to *F*-region heights near the crest of the equatorial anomaly, strong scintillations may be observed at stations near the anomaly crest, because the plasma-density variation is much larger. The time and place of maximum scintillations is highly variable, because the intersection of the bubble with the anomaly crest is a function of the upward and eastward velocities of the bubble, and the westward movement of the anomaly at the velocity of the sunset terminator [*Whalen, 2000*]. In their study, *Chakraborty et al.* [*1999*] used the SI index as a measure of scintillations, instead of the S_4 index, to which it is related [*Secan et al., 1995*]. Examples of the differing patterns of ionospheric-plasma distribution that have a causative connection with the solar activity dependence of scintillation occurrence are displayed in Figures 5 and 6. These figures show the high level of ambient ionization, as represented by the TEC, during the post-sunset period for a sunspot maximum year (1979); while in an year with moderate sunspot number (1984), the ambient ionization decreased to moderate values. During this phase of the solar cycle, more importantly from a scintillation point of view, there is generally no rapid increase in the height of the *F* layer in the post-sunset period, in contrast to the situation depicted in Figure 5 for the year 1979. The dominant role played by electrodynamical processes, in the onset and growth of plasma instabilities in the *F* region of the low-latitude ionosphere, has been confirmed by the results of *Mendillo et al.* [*2001*], obtained using airglow and GPS observations.

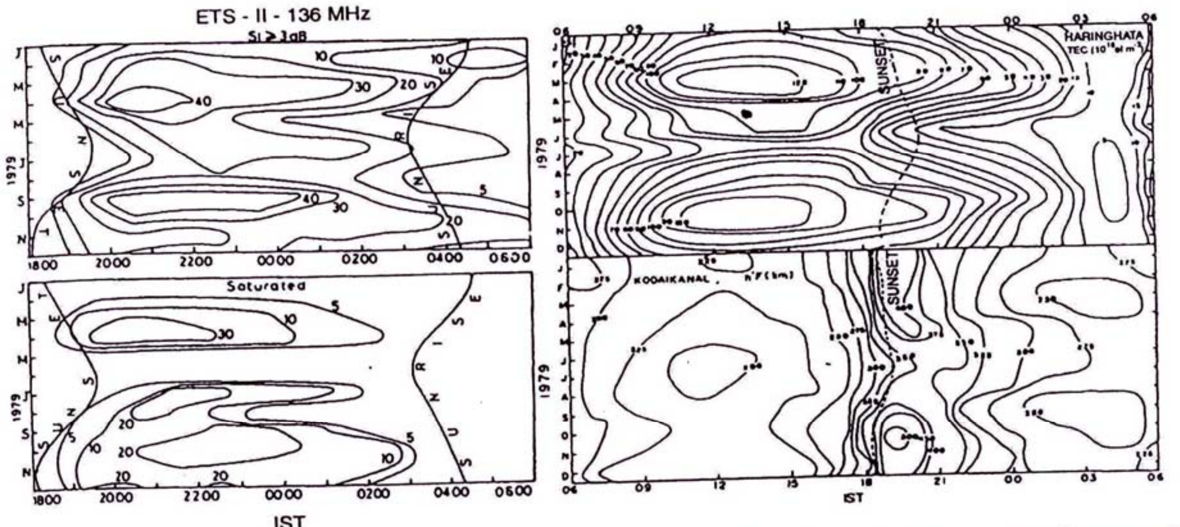

Figure 5. Contours of 136 MHz scintillation occurrence, at SI > 3 dB and saturated levels, near the anomaly crest, as a function of local time and season for the maximum sunspot year 1979. The TEC contours are for the same location. The $h'F$ contours are for a station near the dip equator [after *Chakraborty et al., 1999*].

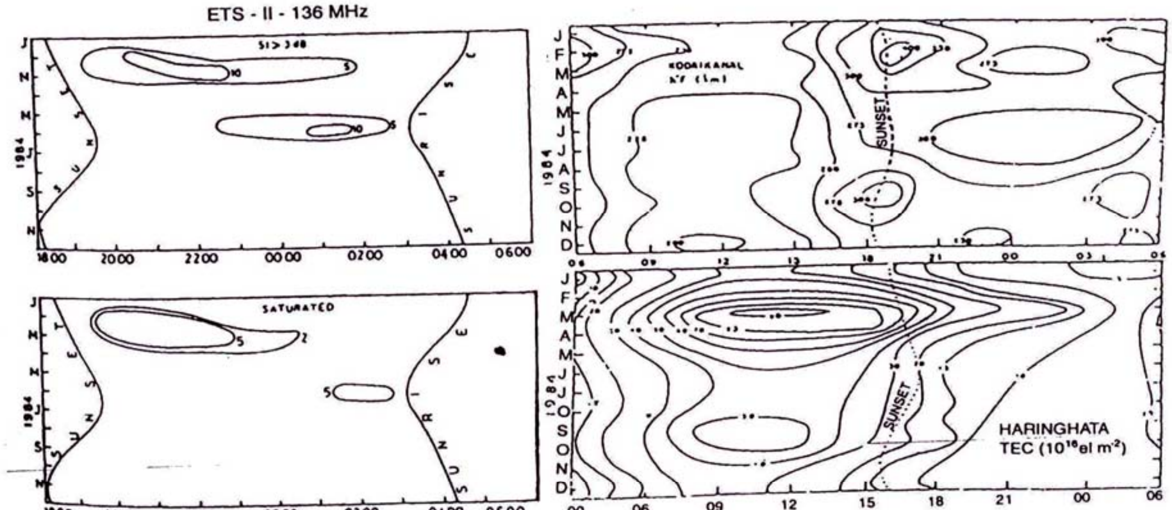

Figure 6. The same as in Figure 5, but for the year 1984, with moderate sunspot numbers [after *Chakraborty et al., 1999*].

4.3.2 Effect of Magnetic Activity

A comprehensive study of the effect of the great magnetic storm of July 15, 2000, on the equatorial ionosphere was carried out by *Basu et al.* [*2001a*]. This used ground-based GPS and geostationary-satellite measurements of TEC and scintillations, and in-situ observations of ion density and ion drift by the sun-synchronous polar-orbiting DMSP satellites, and the ROCSAT-1 satellite in a low-inclination orbit. Results of this study demonstrated that great magnetic storms can create conditions that lead to intense ionospheric irregularities in low-latitude regions, within limited longitudinal ranges. The global coverage offered by such observations – during two major magnetic storms that occurred during the International Space Weather Period of September and October, 1999 – have yielded new insights into the interplay between local-time- (LT) and universal-time- (UT) dominated effects of major magnetic storms on the equatorial ionosphere. These effects could arise from the prompt penetration of electric fields due to an increase or decrease in high-latitude convection, as well as from the ionospheric disturbance dynamo. *Basu et al.* [*2001b*] found that the prompt-penetration electric fields cause VHF/UHF scintillations and GPS TEC variations in the specific longitude sector for which the early evening period corresponds to the time of rapid variation in the Dst index (or its recently available high-resolution one-minute counterpart, the SYM-H index) and maximum Dst phase. This is seen in Figure 7, where the UT variation of the SYM-H index for the period September 22-23, 1999, is displayed in the top panel. The UT variations of the scintillation index, S_4, on 250 MHz signals from two geostationary satellites, Fleetsat-7 (F7) and Fleetsat-8 (F8), recorded at the equatorial station Ancon, during that period, are shown in the bottom two panels. There are two surprising features in this figure. One is the start of scintillations on the 250 MHz signal from the F8 satellite to Ancon, at 2308 UT (1808 LT), which is 15 minutes before the field-line-connected *E*-region (100 km) sunset. The other is the absence of scintillations on the 250 MHz signal from satellite F7 to Ancon, during the evening of September 22-23. The sub-ionospheric intersection point of this signal is 630 km west of the F8 intersection point. These features indicate that onset of scintillations is related to the prompt penetration of eastward electric field, made possible by conductivity gradients near sunset, and that the equatorial prompt penetration at dusk is highly localized in longitude. The effects of the delayed ionospheric disturbance dynamo, and those of decreased magnetospheric convection on post-midnight generation of irregularities, were also seen to be confined to a part of the same longitude range that actively responded to the prompt penetration of electric fields in the early evening sector [*Basu et al.*, *2001b*].

On the basis of their observations at Jicamarca, *Fejer et al.* [*1999*] concluded that the occurrence of early-night spread *F* is significantly less during equinox solar-maximum magnetic disturbances. On the other hand, occurrence of late-night spread *F* was found to peak near solar minimum, decreasing with an increase in solar activity, which was attributed to the large increase of nighttime downward drifts with increasing solar flux [*Fejer et al.*, *1999*]. In a review of the morphology of equatorial *F*-region irregularities during an equinoctial month at solar minimum, *Aarons et al.* [*1999*] reported that on the night of October 22-23, 1996, when a major magnetic storm occurred, GPS data indicated that irregularities were observed over a wide range of longitudes, spanning over 90°. The high-altitude, long-lasting "super-plume," seen on backscatter maps from the Jicamarca radar on this night, must have extended to heights of over 2000 km above the magnetic equator, as indicated by GPS data at off-equatorial locations.

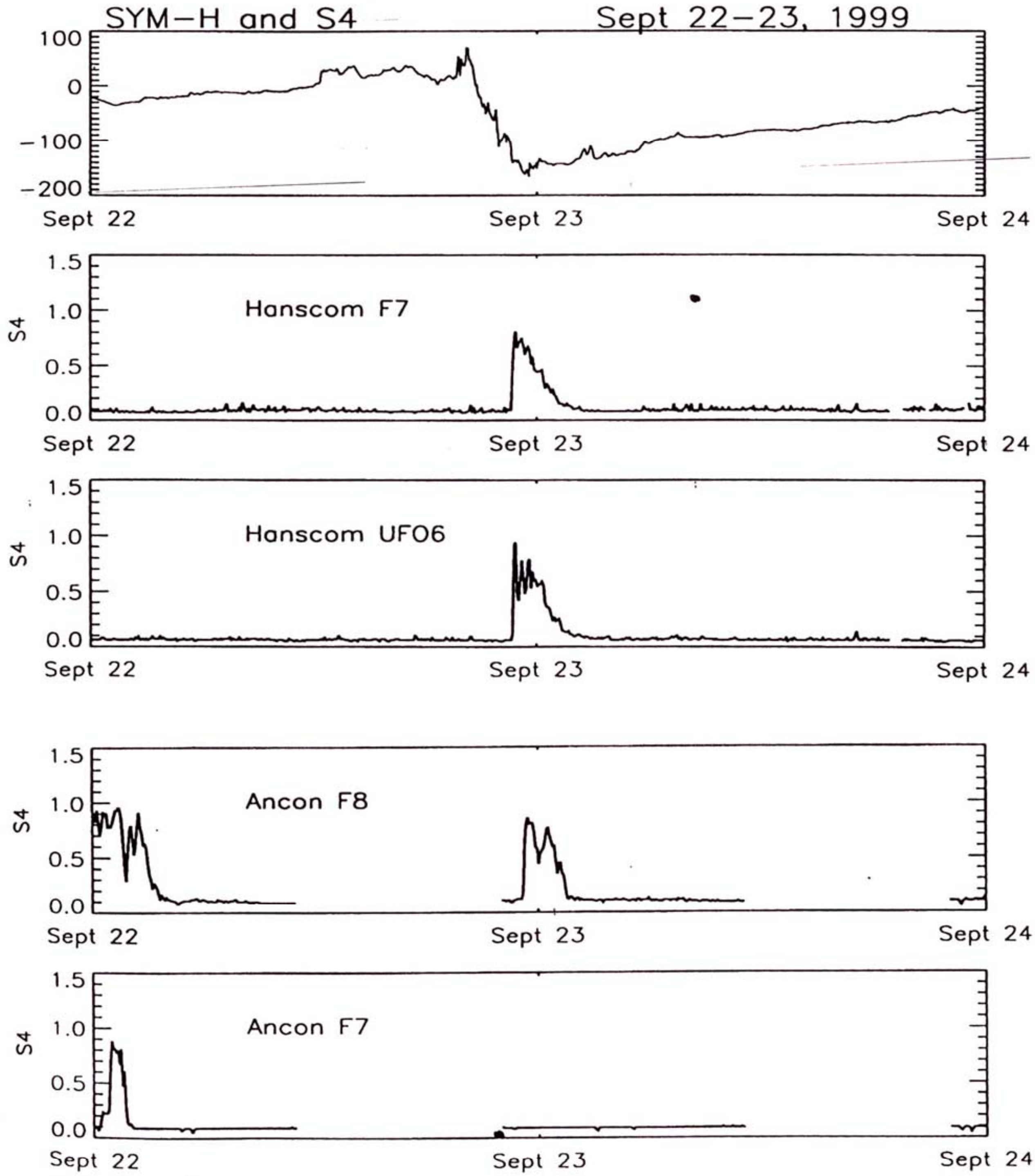

Figure 7. (Top to bottom) Panel 1: The UT variation of high-resolution (one-minute) SYM-H index for the period September 22-23, 1999; Panels 2 and 3: The scintillation index, S_4, for 250 MHz signals from the geostationary satellites Fleetsat-7 (F7) and UFO6 (U6), recorded at the mid-latitude station, Hanscom AFB, MA; Panels 4 and 5: The scintillation index, S_4, for 250 MHz signals from geostationary satellites Fleetsat-7 (F7) and Fleetsat-8 (F8), recorded at the equatorial station, Ancon [after *Basu et al., 2001b*].

4.3.3 Spaced-Receiver Scintillation Observations

There are generally two processes at work in the scattering of electromagnetic waves by a turbulent plasma. The first process is the temporal variation of the scattering eddies in a coordinate system, which moves with the local velocity, and the second is the movement of the irregularities as a whole, with an average velocity. The irregularity drift velocity is a combination of the ambient plasma drift and the $\mathbf{E}\times\mathbf{B}$ drift, due to the perturbation electric field associated with the irregularity. Spaced-receiver observations of scintillations on transionospheric radio waves, transmitted from a geostationary satellite, yield the average speed with which the irregularities drift across the signal path. They also provide estimates of a parameter called the "random velocity," which describes the temporal variation of the irregularities in a coordinate system that moves with the local average velocity. The irregularity drift shows large day-to-day variations in the initial phase of bubble development, which takes place shortly after sunset during magnetically quiet periods [*Kil et al., 2000*; *Palmroth et al., 2000*; *Bhattacharyya et al., 2001*]. During this time interval, the random velocity has relatively high values due to the large variability of the irregularity drift, and declines to smaller values (≤ 20 m/s) after this initial phase. In recent computer simulations of the temporal evolution of equatorial *F*-region bubbles, the behavior of a dynamic background plasma and neutral thermospheric components have been taken into account in the computation of density and plasma velocities in the region of the bubble [*Retterer, 1999*]. The simulations showed that the ranges spanned by the extrema of the upward and eastward velocities in the region of the bubble increase rapidly after local sunset to reach a peak. They then decline more gradually over a period of about an hour, after which the extrema are much closer to the ambient plasma drift. The density structures associated with the bubbles are found to persist long after the velocity structures have been eroded. Ionospheric scintillations recorded at a particular location have contributions from irregularities generated in the region of the signal path, as well as from irregularities that formed earlier at a different location and, with time, drifted onto the path of the signal. Thus, the random velocity gives an indication of the age of the irregularities that produce the observed scintillations, which may be useful in a regional-specification and short-term forecast system [*Groves et al., 1997*]. A magnetically disturbed night may see a resurgence of the random velocity [*Bhattacharyya et al., 1989*] in the post-midnight period, due to a fresh generation of irregularities, when the ambient electric field is reversed from westward to eastward [*Abdu et al., 1997*; *Sastri et al., 2000*; *Burke et al., 2000*].

4.4 MID-LATITUDE IONOSPHERE

Large scale effects at mid-latitudes, of ionospheric storms driven by highly variable solar and magnetospheric energy inputs into the Earth's upper atmosphere, are well documented [*Buonsanto, 1999*]. Space-weather-related ionospheric structures, which can scatter transionospheric radio waves, have generally been found to be less pronounced in the mid-latitudes than in the high- and low-latitude ionospheres. Some recent studies of highly structured TEC signatures, observed at a location in Puerto Rico, have revealed a different response of the mid-latitude ionosphere to strong geomagnetic activity [*Garcia et al., 2000*; *Kelley et al., 2000*; *Makela et al., 2000*]. One such event is shown in Figure 1, where the TEC shows large fluctuations after sunset. It was argued by *Kelley et al.* [*2000*] that these fluctuations are not due to an equatorial "super-plume," reaching a height of 2000 km over the equator from where it mapped to the mid latitude *F*-region. Instead, they suggested that secondary local instabilities gave rise to the sub-structure in the primary wavelike structures, seen in all-sky images using the 630 nm airglow emission. On another night, a severe depletion, which was highly localized in the east-west direction, was found in the TEC measured at the same location in Puerto Rico, using GPS observations [*Makela et al., 2000*]. This depletion was also observed with incoherent-scatter radar. Data, obtained by the DMSP satellite, showed that on this night, very large density fluctuations occurred in the southern mid-latitude ionosphere at a height of 800 km, and these were found within three hours of a jump in Kp from 3 to 6+. According to *Makela et al.* [*2000*], this indicated that the main source of ionospheric disturbance was in the southern hemisphere. The observed effect on the GPS signal received at the northern mid-latitude station was then caused by the mapping of electric fields from the south to the north, and their subsequent mixing with a steep equator-ward gradient in density, which existed in the northern region.

The effects of two major magnetic storms, one on September 22-23, 1999, and the other on October 22, 1999, on the mid-latitude ionosphere, have been recently studied by *Basu et al.* [*2001b*]. The hourly Dst index was −167 nT at 2400 UT on September 22, and −231 nT at ~0700 UT on October 22. The authors showed that the penetration of transient magnetospheric electric fields equator-ward of the shielding region at mid-latitudes, which are known to have good correlation with rapid variations in the Dst index, can cause a large increase of TEC, fluctuations in TEC, and saturated scintillations on a 250 MHz signal. Such developments may have significant impact on GPS-based navigation systems in the mid-latitudes. The second and third panels from the top in Figure 7 show the variation with UT of the scintillation index, S_4, for 250 MHz signals transmitted from two geostationary satellites F7 and UFO-6, and received at a mid-latitude station. The sub-ionosphere (350 km) intersection points for the two signals are very close, such that there is simultaneous onset of scintillations on both signals. *Basu et al.* [*2001b*] considered the impulsive onset of scintillations at $L = 2.8$ to be linked with the appearance of electric fields and plasma gradients in that vicinity. They found that the LT of penetration of the electric field dictates the magnitude of the impact of major magnetic storms on communication and navigation systems operating in this region. At local dusk, an equator-ward motion of the mid-latitude trough was seen, and this gave rise to plasma instabilities driven by the density gradient.

4.5 POLAR CAP/AURORAL IONOSPHERE

4.5.1 Polar-Cap Patch Activity

Space-weather effects on radio wave signals propagating through the high-latitude ionosphere are a direct result of solar-wind-magnetosphere-ionosphere coupling processes. As far as intermediate-scale irregularities in the ionospheric electron density at high latitudes are concerned, the dayside auroral oval may be considered to be the source region and gateway for the transfer of solar-wind energy to the ionosphere. Under active magnetic conditions, the eastward electric field in the dayside auroral oval directs a "tongue of ionization" from the sub-auroral region into the polar cap, which is sliced off into discrete large-scale ionization structures by high plasma flows [*Valladares et al., 1994*]. The convecting patches develop intermediate-scale irregularities by the action of the gradient-drift instability mechanism, and these irregularities may give rise to strong scintillations on radio wave signals [*Basu et al., 1985*; *Kersley et al., 1995*]. Another source of localized intermediate-scale irregularities is the sheared electric field in the cusp/cleft region. The irregularities generated in velocity-shear regions exhibit highly enhanced electric-field fluctuations for a given fluctuation in relative density, compared to that seen in the case of irregularities produced by convective instabilities at high latitudes. The magnitude of electron-density fluctuations is expected to be higher in the region of polar-cap patches, as compared to the velocity-shear regions, since the patches have higher plasma density. Hence, scintillations on transionospheric radio waves, caused by patch-associated irregularities, are expected to be stronger than those due to irregularities produced by velocity shear. The temporal structure of scintillations is also different in the two cases, since enhanced electric-field fluctuations broaden the frequency spectra of scintillations. Under solar-minimum conditions, *Basu et al.* [*1998*] have reported persistent observations of weak amplitude scintillations on a 250 MHz signal during daytime, at about 2° pole-ward of the nominal cusp region. The observed dayside scintillations, which indicated the presence of sub-kilometer-scale-size irregularities, were characterized by generally broad frequency spectra, as expected for irregularities in a turbulent-flow regime. During a major magnetic storm, a drastic change in the pattern of scintillation from the quiet-day pattern of enhanced scintillation activity around magnetic noon, was reported by *Basu et al.* [*1998*]. This was attributed to the station becoming a polar-cap station, due to the expansion of the auroral oval to lower latitudes under magnetically active conditions. This hypothesis was confirmed by optical images, which showed no auroral emission within the entire field of view of the imager. GPS satellite data, recorded at this station, showed the presence of patches with small TEC enhancements only during the major magnetic storm. The high geographic latitude of the cusp in the observation sector resulted in weaker polar-cap patches and associated irregularities. More recent storm-time studies of scintillations in the high-latitude regions showed some of these complexities, which have to be considered in understanding the space-weather effects on transionospheric radio waves in these regions. As far as the use of IGS data on GPS signals to study the density irregularities in the high-latitude ionosphere is concerned, it has to be kept in mind that at these latitudes, the convection speeds may be so large that a sampling period of 30 s for the IGS data yields information on very large scale ($\approx$40 km) fluctuations in the phase, and hence may not provide accurate information about scintillation effects [*Basu et al.*, *1998*].

The morphology of polar-cap patch activity during a one-year period of high solar activity has been studied by *Dandekar and Bullet* [*1999*]. For this investigation, besides monitoring UHF scintillation data from Thule with a corrected geomagnetic latitude (CGL) of 86.0° N, digital ionospheric sounding systems were in operation at two stations with CGL of 86.7° N and 75.2° N, and airglow images were recorded at the first of these two stations. The observations were consistent with the source mechanism for patches discussed above. During the period of observation, the polar-cap patches displayed a strong seasonal dependence, with the highest occurrence in the winter months. The patch occurrence and strength both showed a diurnal behavior, with maximum occurrence around 2200-0200 UT and a minimum around 0600-1100 UT. The patch activity was also seen to be weakly dependent on the magnetic-activity index, Kp, and the results supported the present understanding that the macro-scale, enhanced-density polar-cap patches predominantly occur with the southward turning of the interplanetary magnetic field (IMF). The origin of the patches, their modification by the electric-field structure in the cusp, their interaction with the neutral medium, the meso-scale structuring that gives rise to scintillations, their convection through the polar cap, and their eventual exit into the auroral oval are well documented in a review by *Basu and Valladares* [*1999*]. There is a predominant feeling among researchers in the field of high-latitude plasma structuring that the polar atmosphere alternates between two states, depending on the sign of IMF B_z. However, simultaneous polar-cap patches and sun-aligned arcs have been identified in a single common 1000 km field-of-view of optical and radio instruments, co-located within the northern-hemisphere polar cap. *Valladares et al.* [*1998*] found a polar-cap transition state from a patch-dominated to an arc-dominated pattern in 19 cases, studied during the period 1989-92.

4.5.2 Development of Storm-Time Irregularities

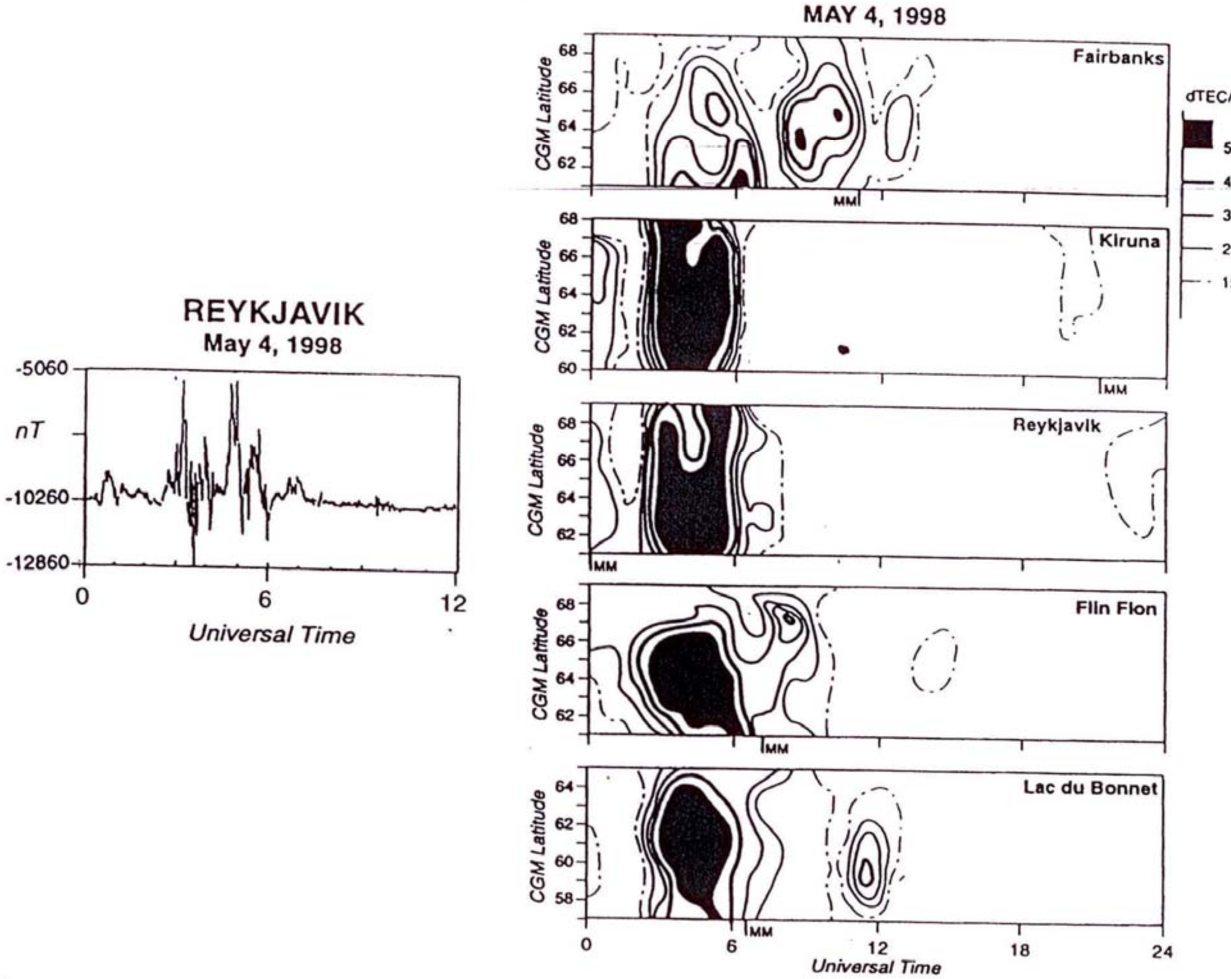

Figure 8. On the left is a magnetogram from Reykjavik, showing large magnetic excursions during a major magnetic storm, with Kp reaching levels of 9- and 8+ during the period 03-09 UT on May 4, 1998. On the right, the dominance of the storm time is seen in the development of irregularities at a number of high-latitude locations, as shown by the variations $d\text{TEC}/dt$ in GPS TEC, during periods of very large magnetic perturbations [after *Aarons et al., 1999b*].

Aarons et al. [*2000*] have carried out the first detailed study of the order of development of ionospheric irregularities at high latitudes during geomagnetic storms, using ultraviolet images (UVI) of the aurora from the polar satellite. These were used in conjunction with differential-phase fluctuations and TEC information from GPS data at a number of sites, magnetometer records, and hemispheric power precipitation. The Kp index is a traditional measure of global magnetic activity, and provides a macro-scale picture, whereas local magnetometer records give an assessment of disturbances on a micro-scale. *Aarons et al.* [*2000*] found a good correlation between the UVI intensity of 170 nm emission, which is sensitive to precipitation at a 100 to 200 km height range, and the intensity of phase fluctuations derived from GPS data. During excursions of the magnetic field, TEC derived from GPS data showed both a general increase over a large area, and increases on a scale of 6 km. Therefore, besides velocity shear, structured precipitation in the 100 km-to-lower-*F*-region heights may also play a role in the development of irregularities in the auroral-oval region [*Erikhimov et al., 1994*; *Aarons and Lin, 1999*]. It was also observed by *Aarons et al.* [*2000*] that two distinct forcing functions are responsible for space-weather effects on transionospheric radio waves recorded in these regions. One of them is determined by storm time, while the other depends on magnetic local time, as seen from the temporal evolution of irregularities that produce phase fluctuations on GPS signals. An example of this is seen during the great magnetic storm that occurred in the period May 1-6, 1998 [*Aarons et al., 1999b*]. During the period 03-09 UT on May 4, when the magnetic perturbation was extremely large, with Kp levels of 9- and 8+, strong phase fluctuations were observed simultaneously all across the auroral zone, even at sites in daylight, as seen in Figure 8. On the other hand, within the storm time, until May 4, the production of irregularities was found to be dominated by the magnetic local time.

4.5.3 Orientation of Irregularities

The role of electric fields in the high-latitude *F*-region in the generation of sub-kilometer-scale irregularities was examined by *Tereshchenko et al.* [*2000*]. This was done by studying the correlation between the electric-field direction, obtained from plasma-flow measurements using the EISCAT incoherent-scatter radar, and orientation of the anisotropic irregularities. The orientation was determined from scintillation measurements on satellite signals by a modified version of the method suggested by *Tereshchenko et al.* [*1999*]. It was found that in nearly all the cases where it was possible to compare the orientation of the irregularities with the *F*-region plasma flow, the orientation was in the flow direction. This suggests that the instability that creates the density fluctuations was driven by the electric field. Since the pattern of scintillation has a significant dependence on the orientation of the signal path with respect to the anisotropic irregularities, space-weather effects on the electric field will also influence scintillations on transionospheric radio waves through this factor.

5. IONOSPHERIC TOMOGRAPHY

The previous sections have described some of the recent results pertaining to space-weather effects on transionospheric radio waves. These are either due to large-scale variations in ionospheric electron density on account of enhancement, as in the case of high-latitude precipitation, or redistribution of ionospheric plasma; or due to generation of sub-kilometer-scale structures by plasma instabilities. *Granat and Na* [*2000*] have developed a novel artificial-neural-network-based computerized ionospheric tomography (CIT) technique, which may be capable of detecting short-term localized disturbances in the ionosphere, such as those associated with space weather effects. The distribution of ionospheric plasma on a large scale also plays an important role in the evolution of the sub-kilometer-scale structures. For instance, in the case of ESF irregularities, which are nearly field-aligned structures, the distribution of plasma all along the geomagnetic field lines that connect the equatorial *F*-region to the conjugate *E* regions affects their development [*Keskinen et al., 1998*; *Bhattacharyya and Burke, 2000*]. The low-latitude ionospheric-plasma distribution is dominated by the equatorial-anomaly (EA) region, at ±15° -20° geomagnetic latitude on both sides of the magnetic-dip equator. The pre-reversal enhancement of eastward electric field in the equatorial region, which has emerged as a crucial factor in the development of ESF, is also the cause of the EA during the evening hours. The onset of ESF has been shown to be closely related to the temporal evolution of the TEC profile as a function of latitude, near sunset [*Valladares et al., 2001*]. Hence, studies of the formation and highly variable nature of EA are very important, and computerized ionospheric tomography (CIT) has emerged as a powerful technique for such investigations [*Andreeva et al., 2000*]. These authors used data from the low-latitude ionospheric-tomography network, which consists of a chain of six stations that receive radio signals transmitted by the Navy Navigation Satellite System (NNSS). The reconstructed ionospheric images have provided unprecedented details of the northern crest of the equatorial anomaly around 121° E. Some of the features revealed by the images – such as the TEC crest being broader and occurring at a lower latitude than the crest in peak electron concentration – have implications for application in satellite-based navigation and surveillance systems. Such results from application of CIT, in conjunction with modeling efforts, will lead to a better understanding of the specific influences of electric fields and neutral winds upon the distribution of plasma during anomaly formation times. Both of these influences are intimately connected with space-weather effects on transionospheric radio waves.

In the mid-latitudes, GPS TEC data and profiles of electron-density measurements, made with an incoherent-scatter radar, have been used as inputs in a CIT algorithm. This reconstructed ionospheric-plasma distributions with data from three Transit-satellite receivers, as part of a combined ionospheric campaign carried out in the Caribbean, centered on Puerto Rico, during June, 1998 [*Bust et al., 2000*]. One of the days during the campaign was magnetically disturbed, with Kp going up to 6+, and staying high for nearly 12 hours. During this period, the ionospheric images showed several depleted structures, not only over the Puerto Rico region, but throughout the Caribbean region, and a sharp plasma boundary near 40° N latitude, with a large extended depletion zone above 40° N. The authors suggest that the penetrating high-latitude electric field, during the magnetically active period, may have swept away the ionization above 40° N, creating conditions for producing a structured mid-latitude zone. Such walls of ionization have been observed at mid-latitudes during high magnetic activity [*Foster and Rich*, *1998*].

At high latitudes, phase-coherent radio signals on 150 and 400 MHz – transmitted by the Navy Ionospheric Monitoring System (NIMS), also known as NNSS satellites, and monitored by a latitudinal chain of four ground-based receivers – have been used to reconstruct the spatial distribution of electron density using the CIT technique [*Berry et al., 2000*; *Pryse et al., 2000a*; *2000b*]. Tomographic images have shown the existence of spatial structures in the afternoon auroral ionosphere that could be related to the precipitation of particles from the magnetosphere. Different regions were identified in particle observations from passes of DMSP satellites, which corresponded to distinct features in the ionospheric plasma. The structures seen between 79° N and 81° N in a tomographic image were found to be within the region of precipitation of boundary-plasma-sheet origin. Further north, a transition took place to a less-structured *F*-layer that corresponded to a region where the precipitation could be classified as being of de-energized-magnetosheath origin [*Berry et al., 2000*]. The effect that the orientation of the IMF has on the distribution of plasma in the polar ionosphere is also a topic that has been investigated using radio tomography, in conjunction with complementary experimental techniques [*Pryse et al., 2000a*]. In another investigation, footprints of magnetopause reconnection were identified in radio-tomographic images of the high-latitude ionosphere, by using well-established ion-dispersion signatures during three DMSP satellite passes [*Pryse et al., 2000b*].

6. CONCLUSIONS

Space-weather effects on transionospheric radio waves fall into two categories: (a) changes in the excess time delay introduced by large-scale variations (> 10 km) in the ionospheric plasma density; and (b) amplitude and phase scintillations caused by the appearance of sub-kilometer structures in the ionospheric plasma, usually due to the growth of a plasma instability. The excess time delay is simply proportional to the STEC along the signal path. In recent years, there have been many studies of space-weather effects on TEC in different regions that use GPS data from a large number of sites. In most studies, the TEC derived from GPS observations has been identified with the ionospheric electron content (IEC). However, there have been a few investigations into the contribution of plasmaspheric electrons to the TEC measured using GPS signals, which is a potential source of error in the estimation of the IEC. These studies include theoretical modeling of the contribution from the protonosphere, and comparison with experimental measurements using GPS and the lower-orbiting NIMS satellite signals. The *F* region of the ionosphere is the most important region for transionospheric radio propagation, since the plasma density is the highest in this region. Hence, there has been a greater emphasis on understanding the response of the ionospheric *F* layer to space-weather variations. As far as large-spatial-scale behavior is concerned, GPS data has provided a wide range of cause-effect scenarios in recent investigations. In particular, geomagnetic activity of a given magnitude, as measured by standard geomagnetic indices, is seen to elicit different responses from the ionosphere in the same region, depending on the local time, season, and solar activity. Given the complexity of the problem, physics-based models of the ambient ionosphere may provide the insight necessary to understand the observed patterns. The recent trend is to develop global-ionospheric-data assimilation models, which will be driven by appropriate inputs derived from various types of data in real time, to improve the ionospheric specification. The most important inputs are the high-latitude convection electric field, auroral currents and particle precipitation, solar radiation, and tides and gravity waves that propagate from below. The availability of simultaneous GPS data from globally distributed sites makes this an important tool for model validation.

Another challenging task is to find the link between space-weather parameters and the characteristics of ionospheric irregularities, including the very basic question of the prediction of the occurrence of these irregularities, which may have a severe impact on transionospheric radio propagation. During the last few years, observations of ionospheric irregularities of various scale sizes – using radar, scintillation techniques, and airglow images, besides in-situ measurements of density and electric-field fluctuations by satellites – have yielded a large amount of information on the characteristics of irregularities under different conditions. Some crucial parameters are now emerging as the key players in the development of the irregularities. Computer simulations of the non-linear evolution of plasma instabilities that give rise to these ionospheric irregularities may, in the near future, yield those characteristics of the irregularities that are of importance from the point of view of forecasting the outage of communication and navigation systems due to scintillations. An understanding of the pattern of evolution of the irregularities, their dynamics, and knowledge of the background ionosphere can be incorporated into an improved regional specification and short-term forecast system.

7. REFERENCES

J. Aarons, M. Mendillo, and R. Yantosca [1997], "GPS Phase Fluctuations in the Equatorial Region during Sunspot Minimum," *Radio Science*, **32**, pp. 1535-1550.

J. Aarons and B. Lin [1999], "Development of High Latitude Phase Fluctuations during January 10, April 10-11, and May 15, 1997 Magnetic Storms," *Journal of Atmospheric and Solar-Terrestrial Physics*, **61**, pp. 309-327.

J. Aarons, M. Mendillo, B. Lin, M. Colerico, T. Beach, P. Kintner, J. Scali, B. Reinisch, G. Sales, and E. Kudeki [1999a], "Equatorial *F* region Irregularity Morphology during an Equinoctial Month at Solar Minimum," *Space Science Reviews*, **87**, pp. 357-386.

J. Aarons, M. Mendillo, and B. Lin [1999b], "The Great Magnetic Storm of May 1998 and its Effect on Phase Fluctuations in the Auroral and Equatorial Regions," in *Proceedings of the Ninth International Ionospheric Effects Symposium*, (available from J.M. Goodman, Radio Propagation Services, Inc., 8310 Lilac Lane, Alexandria, VA22308, USA), pp. 136-143.

J. Aarons, B. Lin, M. Mendillo, K. Liou, and M. Codrescu [2000], "Global Positioning System Phase Fluctuations and Ultraviolet Images From the Polar Satellite," *Journal of Geophysical Research*, **105**, pp. 5201-5213.

M. A. Abdu, J. H. Sastri, J. Mac Dougall, I. S. Batista, and J. H. A. Sobral [1997], "Equatorial Disturbance Dynamo Electric Fields Longitudinal Structure and Spread *F*: A Case Study from GUARA/EITS Campaigns," *Geophysical Research Letters*, **24**, pp. 1707-1710.

E. L. Afraimovich, V. V. Chernukhov, and V. V. Demyanov [2000], "The Updated Ionospheric Delay Model to Improve the Performance of GPS Single Frequency Receivers," *Radio Science*, **35**, pp. 257-262.

E. L. Afraimovich [2000], "GPS Global Detection of the Ionospheric Response to Solar Flares," *Radio Science*, **35**, pp. 1417-1424.

D. N. Anderson, M. Buonsanto, M. Codrescu, D. Decker, C. G. Fesen, T. J. Fuller-Rowell, B. W. Reinisch, P. G. Richards, R. G. Roble, R. W. Schunk, and J. J. Sojka [1998], "Intercomparison of Physical Models and Observations of the Ionosphere," *Journal of Geophysical Research*, **103**, pp. 2179-2192.

E. S. Andreeva, S. J. Franke, K. C. Yeh, and V. E. Kunitsyn [2000], "Some Features of the Equatorial Anomaly Revealed by Ionospheric Tomography," *Geophysical Research Letters*, **27**, pp. 2465-2468.

E. S. Andreeva, S. J. Franke, K. C. Yeh, V. E. Kunitsyn, and I. A. Nesterov [2001], "On Generation of an Assembly of Images in Ionospheric Tomography," *Radio Science*, **36**, pp. 299-309.

N. Aponte, S. A. Gonzalez, M. C. Kelley, C. A. Tepley, X. Pi, and B. Iijima [2000], "Advection of the Equatorial Anomaly over Arecibo by Small-Storm Related Disturbance Dynamo Electric Fields," *Geophysical Research Letters*, **27**, pp. 2833-2836.

G. J. Bailey and N. Balan [1996], "A Low-Latitude Ionosphere-Plasmasphere Model," in R.W. Schunk (ed.), *STEP Handbook in Ionospheric Models*, Logan (Utah), Utah State Univ., pp. 173-206.

Su. Basu, S. Basu, E. MacKenzie, and H. E. Whitney [1985], "Morphology of Phase and Intensity Scintillations in the Auroral Oval and Polar Cap," *Radio Science*, **20**, pp. 347-356.

S. Basu, E. J. Weber, T. W. Bullet, M. J. Keskinen, E. Mackenzie, P. Doherty, R. Sheehan, H. Kuenzler, P. Ning, and J. Bongiolatti [1998], "Characteristics of Plasma Structuring in the Cusp/Cleft Region at Svalbard," *Radio Science*, **33**, pp. 1885-1899.

S. Basu, K. M. Groves, J. M. Quinn, and P. Doherty [1999], "A Comparison of TEC Fluctuations and Scintillations at Ascension Island," *Journal of Atmospheric and Solar-Terrestrial Physics*, **61**, pp. 1219-1226.

Su. Basu and C. Valladares [1999], "Global Aspects of Plasma Structures," *Journal of Atmospheric and Solar-Terrestrial Physics*, **61**, pp. 127-139.

S. Basu, Su. Basu, K. M. Groves, H.-C. Yeh, S.-Y. Su, F. J. Rich, P. Sultan, and M. J. Keskinen [2001a], "Response of the Equatorial Ionosphere in the South Atlantic Region to the Great Magnetic Storm of July 15, 2000," *Geophysical Research Letters*, **28**, pp. 3577-3580.

Su. Basu, S. Basu, C. E. Valladares, H.-C. Yeh, S.-Y. Su, E. MacKenzie, P. J. Sultan, J. Aarons, F. J. Rich, P. Doherty, K. M. Groves, and T. W. Bullett [2001b], "Ionospheric Effects of Major Magnetic Storms during the International Space Weather Period of September and October 1999: GPS Observations, VHF/UHF Scintillations and In-Situ Density Structures at Middle and Equatorial Latitudes," *Journal of Geophysical Research*, **106**, pp. 30389-30413.

T. L. Beach and P. M. Kintner [1999], "Simultaneous Global Positioning System Observations of Equatorial Scintillations and Total Electron Content Fluctuations," *Journal of Geophysical Research*, **104**, pp. 22553-22565.

S. T. Berry, L. Kersley, J. Moen, and W. F. Denig [2000], "Ionospheric Signatures of Magnetospheric Boundaries in the Post-Noon Sector," *Annales Geophysicae*, **18**, pp. 74-80.

A. Bhattacharyya, S. J. Franke, and K. C. Yeh [1989], "Characteristic Velocity of Equatorial *F* Region Irregularities Determined from Spaced Receiver Scintillation Data," *Journal of Geophysical Research*, **94**, pp. 11959-11969.

A. Bhattacharyya, K. C. Yeh, and S. J. Franke [1992], "Deducing Turbulence Parameters from Transionospheric Scintillation Measurements," *Space Science Reviews*, **61**, pp. 335-386.

A. Bhattacharyya [1999], "Deterministic Retrieval of Ionospheric Phase Screen from Amplitude Scintillations," *Radio Science*, **34**, pp. 229-240.

A. Bhattacharyya, T. L. Beach, S. Basu, and P. M. Kintner [2000], "Nighttime Equatorial Ionosphere: GPS Scintillations and Differential Carrier Phase Fluctuations," *Radio Science*, **35**, pp. 209-224.

A. Bhattacharyya and W. J. Burke [2000], "A Transmission Line Analogy for the Development of Equatorial Ionospheric Bubbles," *Journal of Geophysical Research*, **105**, pp. 24941-24950.

A. Bhattacharyya, S. Basu, K. M. Groves, C. E. Valladares, and R. Sheehan [2001], "Dynamics of Equatorial *F* region Irregularities from Spaced Receiver Scintillation Observations," *Geophysical Research Letters*, **28**, pp. 119-122.

W. J. Burke, A. G. Rubin, N. C. Maynard, L. C. Gentile, P. J. Sultan, F. J. Rich, O. de La Beaujardiere, C. Y. Huang, and G. R. Wilson [2000], "Ionospheric Disturbance Observed by DMSP at Middle to Low Latitude during the Magnetic Storm of June 4-6, 1991," *Journal of Geophysical Research*, **105**, pp. 18391-18405.

M. J. Buonsanto [1999], "Ionospheric Storms – A Review," *Space Science Reviews*, **88**, pp. 563-601.

G. S. Bust, D. Coco, and J. J. Makela [2000], "Combined Ionospheric Campaign 1: Ionospheric Tomography and GPS Total Electron Count (TEC) Depletions," *Geophysical Research Letters*, **27**, pp. 2849-2852.

S. K Chakraborty, A. DasGupta, S. Ray, and S. Banerjee [1999], "Long-Term Observations of VHF Scintillation and Total Electron Content Near the Crest of the Equatorial Anomaly in the Indian Longitude Zone," *Radio Science*, **34**, pp. 241-255.

P. J. Chi, C. T. Russell, S. Musman, W. K. Peterson, G. Le, V. Angelopoulos, G. D. Reeves, M. B. Moldwin, and F. K. Chun [2000], "Plasmaspheric Depletion and Refilling Associated with the September 25, 1998 Magnetic Storm Observed by Ground Magnetometers at L = 2," *Geophysical Research Letters*, **27**, pp. 633-636.

B. S. Dandekar and T. W. Bullett [1999], "Morphology of Polar Cap Patch Activity," *Radio Science*, **34**, pp. 1187-1205.

C. V. Devasia, N. Jyoti, K. S. V. Subbarao, K. S. Viswanathan, D. Tiwari, and R. Sridharan [2002], "On the Plausible Linkage of Thermospheric Meridional Winds with the Equatorial Spread F," *Journal of Atmospheric and Solar-Terrestrial Physics*, **64**, pp. 1-12.

L. M. Erikhimov, E. N. Myasinkov, V. I. Kosolapenko, V. A. Cheremnyj, and O. V. Evstatev [1994], "Observations of Total Electron Content, Amplitude and Phase Scintillations in the Auroral Ionosphere," *Radio Science*, **29**, pp. 311-314.

B. G. Fejer, L. Scherliess, and E. R. de Paula [1999], "Effects of the Vertical Plasma Drift Velocity on the Generation and Evolution of Equatorial Spread F," *Journal of Geophysical Research*, **104**, pp.19859-19869.

C. G. Fesen, G. Crowley, R. G. Roble, A. D. Richmond, and B. G. Fejer [2000], "Simulation of the Pre-Reversal Enhancement in the Low Latitude Vertical Ion Drifts," *Geophysical Research Letters*, **27**, pp. 1851-1854.

J. C. Foster and F. J. Rich [1998], "Prompt Mid-Latitude Electric Field Effects during Severe Geomagnetic Storms," *Journal of Geophysical Research*, **103**, pp. 26367-26372.

T. J. Fuller-Rowell, M. V. Codrescu, R. G. Roble, and A. D. Richmond [1997], "How Does the Thermosphere and Ionosphere React to a Geomagnetic Storm?" in B. T. Tsurutani et al. (eds.), *Magnetic Storms*, AGU Monograph 98, Washington DC, American Geophysical Union, pp. 203-225.

F. J. Garcia, M. C. Kelley, J. J. Makela, P. J. Sultan, X. Pi, and S. Musman [2000], "Mesoscale Structure of the Midlatitude Ionosphere during High Geomagnetic Activity: Airglow and GPS Observations," *Journal of Geophysical Research*, **105**, pp. 18417-18427.

R. A. Granat and H. Na [2000], "Estimating Dynamic Ionospheric Changes Without a Priori Models," *Radio Science*, **35**, pp. 341-349.

K. M. Groves, S. Basu, E. J. Weber, M. Smitham, H. Kuenzler, C. E. Valladares, R. Sheehan, E. MacKenzie, J. A. Secan, P. Ning, W. J. McNeill, D. W. Moonan, and M. J. Kendra [1997], "Equatorial Scintillation and Systems Support," *Radio Science*, **32**, pp. 2047-2064.

B. Hofman-Wellenhof, H. Lichtenegger, and J. Collins [1994], *Global Positioning System: Theory and Practice, Third Edition*, New York, Springer-Verlag.

I. Horvath and E. A. Essex [2000], "Using Observations From the GPS and TOPEX Satellites to Investigate Nighttime TEC Enhancements at Mid-Latitudes in the Southern Hemisphere during a Low Sunspot Number Period," *Journal of Atmospheric and Solar-Terrestrial Physics*, **62**, pp. 371-391.

D. L. Hysell [2000], "An Overview and Synthesis of Plasma Irregularities in Equatorial Spread F," *Journal of Atmospheric and Solar-Terrestrial Physics*, **62**, pp. 1037-1056.

N. Jakowski, S. Schluter, and E. Sardon [1999], "Total Electron Content of the Ionosphere during the Geomagnetic Storm on January 10, 1997," *Journal of Atmospheric and Solar-Terrestrial Physics*, **61**, pp. 299-307.

M. C. Kelley [1989], *The Earth's Ionosphere: Electrodynamics and Plasma Physics*, New York, Academic Press Inc.

M. C. Kelley, F. Garcia, J. Makela, T. Fan, E. Mak, C. Sia, and D. Alcocer [2000], "Highly Structured Tropical Airglow and TEC Signatures during Strong Geomagnetic Activity," *Geophysical Research Letters*, **27**, pp. 465-468.

L. Kersley, C. D. Russell, and D. L. Rice [1995], "Phase Scintillation and Irregularities in the Northern Polar Ionosphere," *Radio Science*, **30**, pp. 619- 629.

M. J. Keskinen, S. L. Ossakow, S. Basu, and P. J. Sultan [1998], "Magnetic-Flux-Tube-Integrated Evolution of Equatorial Ionospheric Plasma Bubbles," *Journal of Geophysical Research*, **103**, pp. 3957-3967.

H. Kil, P. M. Kintner, E. R. de Paula, and I. J. Kantor [2000], "Global Positioning System Measurements of the Ionospheric Zonal Apparent Velocity at Cachoeira Paulista in Brazil," *Journal of Geophysical Research*, **105**, pp. 5317-5327.

J. A. Klobuchar [1987], "Ionospheric Time-Delay Algorithm for Single Frequency GPS Users," *IEEE Transactions on Aerospace and Electronic Systems*, **AES-23**, pp. 325-331.

R. Leitinger [1999], "Ionospheric Tomography," in W. Ross Stone (ed.), *The Review of Radio Science 1996-1999*, Oxford, Oxford University Press, pp. 581-623.

N. Lunt, L. Kersley, and G. J. Bailey [1999a], "The Influence of the Protonosphere on GPS Observations: Model simulations," *Radio Science*, **34**, pp. 725-732.

N. Lunt, L. Kersley, G. J. Bishop, A. J. Mazzella, Jr., and G. J. Bailey [1999b], "The Effect of the Protonosphere on the Estimation of GPS Total Electron Content: Validation Using Model Simulations," *Radio Science*, **34**, pp. 1261-1271.

N. Lunt, L. Kersley, G. J. Bishop, and A. J. Mazzella, Jr. [1999c], "The Contribution of the Protonosphere to GPS Total Electron Content : Experimental Measurements," *Radio Science*, **34**, pp. 1273-1280.

N. Lunt, L. Kersley, G. J. Bishop, A. J. Mazzella, Jr., and G. J. Bailey [1999d], "The Protonospheric Contribution to GPS Total Electron Content: Two-Station Measurements," *Radio Science*, **34**, pp. 1281-1285.

B. MacPherson, S. A. Gonzalez, X. Pi, M. Kelley, G. J. Bailey, M. P. Sulzer, G. Hajj, M. Buonsanto, and C. Wang [2000], "Comparison Between SUPIM Simulations and Measured TEC for the January, 1997 Storm," *Geophysical Research Letters*, **27**, pp. 2845-2848.

J. J. Makela, S. A. Gonzalez, B. MacPherson, X. Pi, M. C. Kelley, and P. J. Sultan [2000], "Intercomparisons of Total Electron Content Measurements Using the Arecibo Incoherent Scatter Radar and GPS," *Geophysical Research Letters*, **27**, pp. 2841-2844.

J. J. Makela, M. C. Kelley, J. J. Sojka, X. Pi, and A. J. Mannucci [2001], "GPS Normalization and Preliminary Modeling Results of Total Electron Content During a Mid Latitude Space Weather Event," *Radio Science*, **36**, pp. 351-361.

A. J. Mannucci, B. D. Wilson, D. N. Yuan, C. M. Ho, U. J. Lindqwister, and T. F. Runge [1998], "A Global Mapping Technique for GPS-derived Ionospheric Total Electron Content Measurements," *Radio Science*, **33**, 565-582.

A. J. Mannucci, B. A. Iijima, J. J. Lindqwister, X. Pi, L. Sparks, and B. D. Wilson [1999], "GPS and Ionosphere," in W. Ross Stone (ed.), *The Review of Radio Science 1996-1999*, New York, Oxford University Press, pp. 625-665.

M. Mendillo, B. Lin, and J. Aarons [2000], "The Application of GPS Observations to Equatorial Aeronomy," *Radio Science*, **35**, pp. 885-904.

M. Mendillo, J. Meriwether, and M. Biondi [2001], "Testing the Thermospheric Neutral Wind Suppression Mechanism for Day-to-day Variability of Equatorial Spread F," *Journal of Geophysical Research*, **106**, pp. 3655-3663.

M. Palmroth, H. Laasko, B. G. Fejer, and R. F. Pfaff [2000], "DE 2 Observations of Morningside and Eveningside Plasma Density Depletions in the Equatorial Ionosphere," *Journal of Geophysical Research*, **105**, pp. 18429-18442.

X. Pi, A. J. Mannucci, U. J. Lindqwister, and C. M. Ho [1997], "Monitoring of Global Ionospheric Irregularities Using the Worldwide GPS Network," *Geophysical Research Letters*, **24**, pp. 2283-2286.

S. E. Pryse, A. M. Smith, I. K. Walker, and L. Kersley [2000], "Multi-Instrument Study of Footprints of Magnetopause Reconnection in the Summer Ionosphere," *Annales Geophysicae*, **18**, pp. 1118-1127.

S. E. Pryse, A. M. Smith, L. Kersley, I. K. Walker, C. N. Mitchell, J. Moen, and R. W. Smith [2000], "Multi-Instrument Probing of the Polar Ionosphere under Steady Northward IMF," *Annales Geophysicae*, **18**, pp. 90-98.

J. A. Ratcliffe [1956], "Some Aspects of Diffraction Theory and Their Application to the Ionosphere," *Reports on Progress in Physics*, **19**, pp. 188-267.

J. M. Retterer [1999], "Theoretical Model for Fast Equatorial Bubbles," in *Proceedings of the Ninth International Ionospheric Effects Symposium*, (available from J. M. Goodman, Radio Propagation Services, Inc., 8310 Lilac Lane, Alexandria, VA22308, USA), pp. 688-691.

A. Rocken, J. M. Johnson, J. J. Braun, H. Kawawa, Y. Hatanaka, and Imakiire [2000], "Improving GPS Surveying with Modeled Ionospheric Corrections," *Geophysical Research Letters*, **27**, pp. 3821-3824.

J. H. Sastri, N. Jyoti, V. V. Somayajulu, H. Chandra, and C. V. Devasia [2000], "Ionospheric Storm of Early November 1993 in the Indian Equatorial Region," *Journal of Geophysical Research*, **105**, pp. 18443-18455.

J. A. Secan, R. M. Bussey, E. J. Fremouw, and S. Basu [1995], "An Improved Model of Equatorial Scintillation," *Radio Science*, **30**, pp. 607-617.

E. D. Tereshchenko, B. Z. Khudukon, M. O. Kozlova, and T. Nygren [1999], "Anisotropy of Ionospheric Irregularities Determined from the Amplitude of Satellite Signals at a Single Receiver," *Annales Geophysicae*, **17**, pp. 508-518.

E. D. Tereshchenko, B. Z. Khudukon, M. O. Kozlova, O. V. Evstafiev, T. Nygren, M. T. Rietveld, and A. Brekke [2000], "Comparison of the Orientation of Small-Scale Electron Density Irregularities and *F* Region Plasma Flow Direction," *Annales Geophysicae*, **18**, pp. 918-926.

C. E. Valladares, S. Basu, J. Buchau, and E. Friis-Christensen [1994], "Experimental Evidence for the Formation and Entry of Patches Into the Polar Cap," *Radio Science*, **29**, pp. 167- 194.

C. E. Valladares, K. Fukui, R. Sheehan, H. C. Carlson, and T. Bullett [1998], "Simultaneous Observations of Polar Cap Patches and Sun-Aligned Arcs during Transitions of the IMF," *Radio Science*, **33**, pp. 1829-1845.

C. Valladares, S. Basu, K. Groves, M. P. Hagan, D. Hysell, A. J. Mazzella, Jr., and R. E. Sheehan [2001], "Measurement of the Latitudinal Distribution of Total Electron Content During Equatorial Spread F Events," *Journal of Geophysical Research*, **106**, pp. 29133-29152.

P. A. Webb and E. A. Essex [2000], "An Ionosphere-Plasmaspheric Global Electron Density Model," *Physics and Chemistry of the Earth (C)*, **25(4)**, pp. 301-306.

J. A. Whalen [2000], "An Equatorial Bubble: Its Evolution Observed in Relation to Bottomside Spread F and to the Appleton Anomaly," *Journal of Geophysical Research*, **105**, pp. 5303-5315.

K. C. Yeh and C. H. Liu [1979], "Ionospheric Effects on Radio Communication and Ranging Pulses," *IEEE Transactions on Antennas and Propagation*, **AP-27**, pp. 747-751.

K. C. Yeh and C. H. Liu [1982], "Radio Wave Scintillations in the Ionosphere," *Proceedings of IEEE*, **70**, pp. 324-360.